Interference characterization in underlay cognitive networks with intra-network and inter-network dependence

Samuel D. Okegbile, *Student Member, IEEE,* Bodhaswar T. Maharaj, *Senior Member, IEEE,* and Attahiru S. Alfa, *Member, IEEE*

Abstract—Interference modeling in cognitive radio network is important to ensure adequate coverage in the network. A reliable interference model, however, depends on accurately characterizing the distribution of users. In this paper, the dependence between primary and secondary networks is examined in order to capture more system parameters related to system characterization. Hence, two cases are considered – primary user (PU) interference control and PU with secondary user (SU) interference control mechanisms. Under PU interference control, distributions of PUs follow the Matern hard core process while the distribution of SUs follow the Poisson hole process (PHP). However, under PU with SU interference control, the distribution of active SUs follow a modified PHP. Bound and approximate expressions were derived for coverage probability at both primary and secondary networks, while simple yet accurate expressions were obtained to depict the number of simultaneous active users supported for the two cases. The tight closeness between the bound and the approximate expressions shows the reliability of the presented theoretical analysis. Furthermore, the bipolar network model assumption was relaxed while the case of independence assumption among users was also considered. Numerical result showed close tightness when the bipolar network model assumption was relaxed while the independence assumption was shown to overestimate users' coverage probability.

Index Terms—Channel capacity, Cognitive radio, Coverage probability, Interference modelling, Poisson hole.

1 Introduction

Cognitive radio networks (CRN) continue to receive a lot of attention because of its capability to eliminate the limitations of the traditional grid model in wireless communications. In heterogeneous CRN, unlicensed devices are allowed to transmit on licensed channels as long as their transmissions do not generate excessive interference with the activities of the licensed devices. These unlicensed devices are known as secondary users (SUs), otherwise called cognitive users, and are expected to ensure that their activities do not disrupt the activities of the primary users (PUs), making a level of cognition important in the secondary network. The licensed devices, on the other hand, commonly referred to as the PUs in CRN, are licensed to use their assigned channels with limited (if any) restriction and do not normally contend to use such assigned channels, unlike secondary networks. The possible spectrum reuse resulting from the relationships between these PUs and SUs is now paving the way for more opportunities in the domain of wireless networks and communications.

Three CRN paradigms have been widely considered in the literature, namely overlay [1]–[3], underlay [4]–[9] and hybrid [10] paradigms. In the overlay model, SUs are allowed to make use of the PUs' assigned channels when PUs' channels are idle. This means a typical SU must be able to predict the activities of the PU of its selected channel so as to vacate such a channel before the arrival of the PU. In the underlay model, SUs are allowed to transmit on PUs' channels as long as their transmissions do not cause excessive disruption of the activities of the PUs. This model has less implementation complexity when compared with the other paradigms and is widely considered in the literature. The hybrid model integrates the characteristics of both overlay and underlay, but is considered less often because of the complexity involved.

As users begin to make use of channels under CRN, interference becomes the most important challenge in both primary and secondary networks. There are mainly two possible forms of interference – inter-network and intra-network interference. This interference, if not well managed, can derail the essence of CRN. Because of its importance, significant attention has been paid to interference management and control in past decades. Preliminary efforts have considered the use of the traditional grid model to characterize interference in CRN. This method, however, suffers from many limitations, such as the unrealistic assumptions required to make the model tractable, leading to inaccurate results. Interference was successfully managed using hexagonal grid models, but these also suffer from scalability issues when multiple users are considered and are not useful in enhancing spectrum efficiency because of their inability to model the locations of users in more practical terms. Hence, stochastic geometry (SG) is now being widely considered in

- *S.D. Okegbile is with Department of Electrical, Electronic and Computer Engineering, University of Pretoria, South Africa. E-mail: samokegbile@gmail.com.*
- *B.T. Maharaj is with Department of Electrical, Electronic and Computer Engineering, University of Pretoria, South Africa. E-mail: sunil.maharaj@up.ac.za.*
- *A.S. Alfa is with Department of Electrical and Computer Engineering, University of Manitoba, Canada and Department of Electrical, Electronic and Computer Engineering, University of Pretoria, South Africa. E-mail: attahiru.alfa@up.ac.za.*

wireless communications networks [4], [11]–[13].

SG provides various solutions that are useful in describing and deriving statistical properties of a random collection of points in d-dimensional space. Point processes are the most important element of SG [14] and can be described as a finite random collection of points in some measured space that are useful in modeling spatial locations of nodes in wireless networks. The most popular point process is the Poisson point process (PPP), which has been extensively adopted in the literature owing to its tractability. Other point processes include the binomial point process and Matern hard core point process (MHCP), which have been considered less often owing to the lack of a probability generating function for such assumptions, while the Poisson cluster process (PCP) is complex and intractable. Because of the need to produce tractable, yet accurate models that characterize interference among users, several assumptions and simplifications are normally resorted to. These simplifications in most cases do not depict the characteristics of real-life systems, hence modeling interference in CRN remains an open issue.

In order to reduce intra-network interference in the primary network, channels are normally assigned to PUs with a considerable level of repulsion among users. These repulsions have been implemented as protection zones or exclusion regions in the primary network and are now being extended to secondary networks to guarantee SUs quality of service (QoS). In PUs' protection zones, SUs are not allowed to transmit, as their transmissions will cause interference in the primary network. Detection of these protection zones is known to be aided by two common detection mechanisms: distance-based and threshold-based detection mechanisms. In distance-based protection zones [5], PU protection zones are determined by SUs through estimations of the distance between a typical secondary transmitter and the tagged primary receiver or primary transmitter depending, on whether the protection zone is receiver-centric or transmitter-centric. A similar process is followed to avoid interference with currently transmitting SUs. In a threshold-based protection zone [2], secondary transmitters rely on the sensed signal threshold to determine the protection zones.

With both intra-network and inter-network interference management and control now being considered, modeling distributions of PUs and SUs become more complicated, causing the derivation of expressions for various performance metrics of interest, such as coverage probability, throughput and spectral efficiency, less tractable and difficult to solve. To avoid this difficulty, PUs and SUs are mostly assumed to be distributed according to independent homogenous PPP (HPPP). With such an assumption, exact or approximate closed-form expressions for performance metrics of interest can be obtained. Such an assumption, however, fails to represent the actual characteristics of practical systems and other point processes, such as Poisson hole process (PHP), PCP and MHCP, are now being considered.

1.1 Related Work

Distribution of users in a wireless communications network is an important factor when modeling interference and it is not surprising that the area continues to attract a lot of interest from researchers. While a large body of literature exists on the application of SG in cellular communication networks [15], [16], relatively few publications on SG-based interference modeling in CRN exist at present. The uniqueness of CRN, however, makes it practically impossible to completely adopt the use of cellular network models in CRN, as these networks are different. In CRN, unlicensed users are allowed to make use of licensed bands provided they do not cause harmful interference with the activities of the licensed users. This notion of priority, however, does not exist in cellular networks, as both sets of users are licensed to use the spectrum [15]. Meanwhile, if the objectives of the CRN are carefully determined, the cellular network models can be adapted with little modification. Hence, we also review some useful efforts that have been made in other wireless networks, such as cellular networks and device-to-device networks in this section.

In CRN, the distribution of PUs has been modeled as HPPP while SUs were assumed to follow independent HPPP [2], [3], [17]–[21]. However, this assumption does not actually capture the possible minimum distance between users in the network and two or more users can be arbitrarily closer to one another than is possible in the real system, leading to interference in the network. Hence, the introduction of protection regions becomes a useful approach. The introduction of exclusion regions, however, presents some complexities in the system modeling, leading to various assumptions and simplifications in the literature that are necessary to reduce such complexities. In [21], exclusion zones were implemented on both primary and secondary networks under the assumption that both PUs and SUs are distributed according to independent HPPP. Similar to [21], the authors in [17] also implemented protection zones in both networks with the observation that active secondary users now follow an unknown distribution, which is approximated as a PPP, while also assuming that active secondary transmitters have zero density inside PUs protection zones, an assumption which may underestimate interference in the network. Secondary transmitters within the protection zones of other primary receivers except the tagged primary receiver were further treated as active. With the introduction of exclusion regions, active PUs and SUs are no longer distributed according to independent HPPP as the locations of active SUs are not totally independent of the locations of active PUs. A better distribution that captures more system parameters is therefore imperative.

In an effort to capture more system parameters, the distributions of PUs and SUs were modeled as PPP and PHP (a distribution that captures distributions of SUs located outside PUs' protection regions) respectively in [5]. Similarly, PUs and SUs were assumed to follow the PPP and an extended Matern point process in [18]. However, since the probability generating functionals (PGFL) of PHP and the Matern point process are unknown, PHP was approximated using first and second order statistics [5] while the extended Matern point process in [18] was also approximated as a log-normal distribution.

Finding suitable distributions for users is not only limited to CRN, and is also necessary for heterogeneous cellular networks where macro base stations (MBS) and pico base

stations (PBS) are distributed in such a way that both macro and pico users can make use of the spectral resources with limited intra-tier and inter-tier interference. When only intra-tier dependence is considered, MBS were assumed to follow PPP, while PBS were modeled as PHP [22], [23]. However, in the case of both inter-tier and intra-tier dependence, MBS were assumed to follow PPP, though PBS now follows the Matern cluster process (MCP) [23]. Also, a two-tier heterogenous network where first-tier devices can be deployed to either mitigate interference or extend the coverage region was considered in [24]. With only intra-tier interference management, the distributions of transmitters in the first and second-tier networks were modeled as a Poisson hard core process (PHCP) and a PPP respectively, while second-tier transmitters were said to follow a Poisson hard-core hole process (PHCHP) when inter-tier interference is considered. PHP was also used to model distributions of users in a single-tier network [9], [25]. In device-to-device network [26], PHP was used to model devices involved in device-to-device communication while cellular users were said to follow PCP.

In this work, exclusion regions are placed around all PUs within which no secondary transmitter is allowed to transmit following conventional orthogonal medium access (OMA) technique. Hence, secondary transmitters inside PUs' exclusion regions are immediately deactivated to protect the activities of PUs. We later extended this method to show that the obtained analysis can be adapted to non-orthogonal medium access (NOMA) based CRN with little modifications. In order to mitigate interference at the secondary network, exclusion regions are also introduced around active SUs. Contending SUs are therefore expected to ensure that they are not within the exclusion zones of other active SUs. In summary, for a typical SU to be eligible to transmit, it must be outside the protection zones of both active PUs and currently active SUs. As a result of these constraints, the locations of active SUs are not independent of the locations of active PUs, as mostly assumed. The inter-network dependence between PUs and SUs, however, means that an exact derivation of the expressions for coverage probability and the number of simultaneous active users supported are difficult to obtain. Because of the suitability of PHP to model users in more practical terms, its usage has been adopted in the wireless network [9], CRN [5], [17] and cellular network [22], [23]. However, since there is no known probability generating functional for it, PHP was approximated by PPP in [17], while intra-network interference in the secondary network was neglected in [5]. Its suitability has, however, been demonstrated in [9], [22], [23]. Hence, we model the locations of active SUs using PHP and a modified PHP while also relaxing some commonly made assumptions in CRN.

1.2 Contributions

The main objective of this paper is to characterize interference in CRN in more practical terms while also investigating the behavior of the network when some commonly made assumptions and simplifications are relaxed. Hence two cases were considered in this paper: The PU interference control mechanism and the PU with SU interference control mechanism. The key contributions of this paper are summarized as follows:

- Dependence in CRN: With protection zones around each PU, the distributions of PUs was shown to follow MHCP, while the distributions of SUs follow PHP. We then adopted the usage of protection zones at the secondary network similar to the case of PUs. In this case, a typical SU is not permitted to transmit in active PUs' protection zones and currently active SUs' protection zones. With intra-network and inter-network dependence, distributions of active SUs now follow a modified version of PHP. We derive tight bound expressions for both coverage probability and the number of simultaneous active users supported in the two cases and present the approximations for coverage probabilities due to the difficulty in obtaining closed-form expressions. We also show that our analysis can be adapted to NOMA based CRN with little modifications.
- Randomizing distances between transmitting pair: Next, we relax the bipolar network model assumption, meaning a typical transmitter and its corresponding pair receiver are separated by an unknown random distance. We derive tight bound expressions for the cases considered and compare the result with cases where the bipolar network model is assumed. We present the results and draw a conclusion from the interesting results, which show that the bipolar network model assumption is a safe assumption.
- Independence in CRN: For the purpose of comparison, we also derive closed-form expressions for the two cases considered in this paper under the assumptions of independence among users. In this case, the expressions for PHP and the modified version of PHP obtained after independent thinning are presented and compared with the case of dependence. We then evaluated effects of protection zones around primary and secondary networks on both spectral efficiency and coverage probability.
- Optimization of the number of simultaneous active users supported: The number of simultaneous active users supported is an important measure that describes the essence of CRN. We first obtained simple yet accurate expressions for this metric. Because coverage probabilities depend heavily on the radius of protection zones in both primary and secondary networks, while an increase in protection zones also means fewer channels are available for cognitive users, we optimized the number of simultaneous active users supported so as to obtain an optimal protection zone radius that will guarantee the required coverage. Thus, at any given coverage constraints, the average SU intensity can be determined.

The rest of this article is organized as follows: In Section 2, we present network models for the two cases considered, while we also derive bounds and approximate expressions for the performance metric of interest. Section 3 presents the optimization of the number of simultaneous active users supported, while in Section 4, we relax the bipolar network model assumption in order to investigate the behavior of

TABLE 1
Common notations used

Notation	Definition
Φ_p, λ_p	Point process and the intensity of the baseline PUs
Φ_p^1, λ_p^1	Point process and the intensity of the active PUs
Φ_s, λ_s	Point process and the intensity representing baseline SUs
Φ_s^1, λ_s^1	Point process and the intensity representing active SUs under PU interference control
Φ_s^{11}, λ_s^{11}	Point process and the intensity representing active SUs under PU with SU interference control
r_p	The distance between a typical primary transmitter and its corresponding receiver
r_s	The distance between a typical secondary transmitter and its corresponding receiver
P_p	Primary user transmission power
P_s	Secondary user transmission power
$b(a,r)$	A disk of radius r centred on point a

CRN further. The case of independent thinning is considered in Section 5, while numerical simulations of the presented approaches are presented in Figure 6. Section 7 concludes the paper and offers suggestions for future work. The definitions of some of the notations used in this paper are presented in Table 1.

2 Network Model

Considering a typical CRN where PUs are distributed according to a homogeneous PPP (HPPP) Φ_p of intensity λ_p, $\forall x_i^p, ..., x_n^p \in \Phi_p$ with x_i^p representing the i^{th} PU, as shown in Fig. 1a. Since channels assignments are normally assigned to PUs in such a way that there is limited intra-network interference, PUs are not actually distributed according to HPPP where two or more users can be arbitrarily close to one another, resulting in excessive interference in the network. A slight modification of Fig. 1a through dependent thinning of PPP to reflect more practical system parameters means, PUs now follow a distribution similar to the MHCP as shown in Fig. 1b where hard core holes (called exclusion zones or protection regions) of radius R were carefully carved out to represent more realistic PUs distribution. By this, two or more PUs cannot be arbitrarily close to one another. However, PUs are not always transmitting on their assigned channels and their transmission can be modelled using two state Markov chain model [27] where a typical PU x_k^p activities can be represented as

$$\zeta_{i,c} = \begin{cases} 0 & : \text{PU is inactive} \\ 1 & : \text{PU is active,} \end{cases} \tag{1}$$

where $\zeta_{i,c}$ depicts the activity of x_k^p on channel c, $\forall c = \{1, ..., n_c\}$. Given that τ_k and ϱ_k are the unique transition probabilities of PU on a particular channel c representing the probability of transition from inactive to active and the probability of transition from active to inactive respectively, then PUs activities on such channel c can be summarized in terms of probability as

$$P = \begin{cases} \frac{\tau_k}{\tau_k+\varrho_k} : \zeta_{i,c} = 1 \\ \frac{\varrho_k}{\tau_k+\varrho_k} : \zeta_{i,c} = 0. \end{cases} \tag{2}$$

For simplicity, let $p_a = \frac{\tau_k}{\tau_k+\varrho_k}$, then $\frac{\varrho_k}{\tau_k+\varrho_k} = 1 - p_a$.

Considering a typical primary receiver (y_k^p) centered at the origin and its corresponding transmitter located at a radius $r_p < R$ with PU protection region of radius R centered at the primary receiver following bipolar network model, the probability that such primary transmitter is active is given as p_a. A typical primary receiver (PR) is associated with the primary transmitter (PT) that generates the strongest average received power at the PR. This is given as $P_{tagged} = \arg\max_{x_i^p} E[P_p h_X ||x_i^p||^{-\alpha}]$ where P_p, h_X and $||x_i^p||^{-\alpha}$ represent the PU transmit power, channel gain between the primary transmitter-receiver pair and Euclidean distance between primary transmitter-receiver pair respectively. Note that this relationship follows Rayleigh fading assumption with all PTs transmitting with the same transmit power. The PT with the strongest average received power at the typical PR is therefore the closest PT. The relationship is the same for any secondary transmitter and receiver pair.

The protection region of radius R centered at the PR under the bipolar network model assumption where a typical transmitter is at a distance r_p from its pair receiver is given as [5];

$$R = r_p\Big(\theta_p\Big(\frac{\zeta P_s}{P_p}\Big)\Big)^{1/\alpha}, \tag{3}$$

where ζ is a design factor and θ_p represents the signal-to-noise plus interference ratio (SINR) threshold for primary transmission. Due to the non-availability of any known probability generating functional for MHCP, we obtained an approximation of MHCP for the distribution of active PUs Φ_p^I of intensity λ_p^I. Hence, we approximate the distribution of PUs as a HPPP. This approximation has been validated in [5], [17]. By Slivnyak's theorem, conditioned on a typical active PU $x_k^p \in \Phi_p^1$, other PUs can be said to follow HPPP Φ_p^1 with intensity $\lambda_p^1 = \lambda_p \rho p_a$, where $\rho = \exp(-\lambda_p \pi R^2)$ represents the repulsion between PUs.

Similarly, SUs are allowed to transmit on licensed channels except within PUs exclusion regions in order to avoid interference at the primary network. As a result, the distribution of eligible SUs (SUs that are outside the protection zones of PUs) as shown in Fig. 1c are better represented as PHP Φ_s^I of intensity $\lambda_s^1 = \lambda_s \rho p_b$. In this case, $\rho = \exp(-\lambda_p \pi R^2)$ is the probability that a typical secondary transmitter (ST) is not located inside any PU exclusion region and p_b is the probability that ST decides to transmit. Furthermore, to avoid intra-network interference in the secondary network, protection zones of radius d are also introduced among SUs as shown in Fig. 1d. In this case, no two active SUs can be arbitrarily close to one another as well. For any SU to be active, such SU has to be eligible while also not located in any of the currently

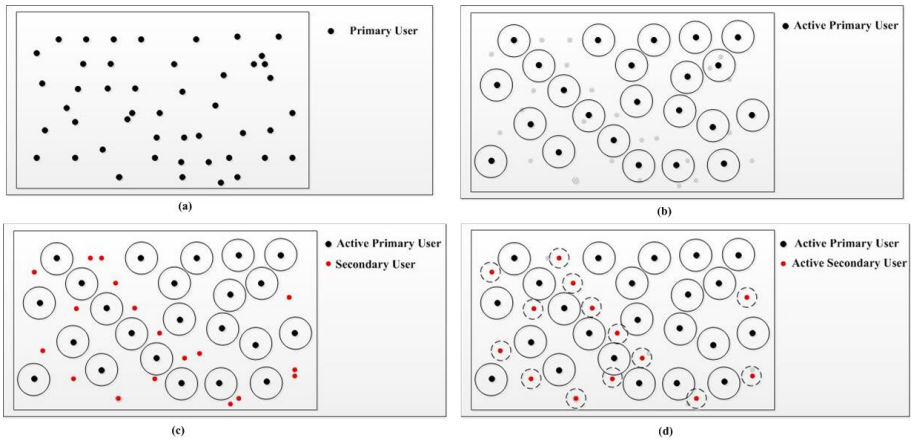

Fig. 1. Dependence in CRN users' distributions

transmitting SU exclusion zone. With this, the distribution of active SUs can be said to follow a modified PHP (mPHP) Φ_s^{II} of intensity λ_s^{II}. This is based on the fact that, other users (when priority is neglected) conditioned on a typical SU ($x_k^s \in \Phi_s^{II}$) can be said to follow PHP. Based on this, SUs that do not satisfy channel access requirements are not allowed to proceed to channel access, but will have to wait for a particular period before transmission upon suitable channel availability.

The distribution of SUs can be summarized as follows: Assuming that SUs are initially distributed according to independent HPPP Φ_s with intensity λ_s, for each SU to access a channel, it passes through two stages which are first and second eligibility stages. In first eligibility stage, a typical SU (say x_k^s) confirms whether it is not within any PU exclusion region. The PU exclusion zone is given as

$$\Xi_R = \bigcup_{y_k^p \in \Phi_p^I} b(y_k^p, R). \tag{4}$$

Eligible SUs Φ_s^I with intensity λ_s^I are therefore distributed according to PHP given as $\Phi_s^I = \{x_k^s \in \Phi_s : x_k^s \notin \Xi_R\} = \Phi_s \backslash \Xi_R$. In the second eligibility stage, x_k^s confirms whether it is not within any currently active SU exclusion region. Similar to (4), SUs exclusion regions can be expressed as

$$\Xi_d = \bigcup_{y_k^s \in \Phi_s^{II}} b(y_k^s, d). \tag{5}$$

Active SUs Φ_s^{II} with intensity $\lambda_s^{II} = \lambda_s^I \exp(-\lambda_s \pi d^2)$ can therefore be represented as a mPHP, which can be represented as $\Phi_s^{II} = \{x_k^s \in \Phi_s : x_k^s \notin \Xi_R \cap \Xi_{d \backslash x_k^s}\}$.

We considered two CRN cases in this paper: PU interference control and PU with SU interference control. Although, all SUs were considered to transmit with equal transmission power in [5], [17], [22], [23], [28], [29], SUs should have the ability to control the transmission power in the underlay cognitive radio networks so as to control the interference to the PUs. Hence, we considered SUs to be under power control scheme [8] given as

$$P_i = \begin{cases} P_s, & \text{if } P_s^I \leq P_s^{max} \\ 0, & \text{otherwise,} \end{cases} \tag{6}$$

where P_s^{max} is the SUs maximum allowable transmission power and P_s^I is the average received power from a typical ST in the presence of channel fading and path loss. Optimization of SUs transmission powers has been discussed in [30] - [33].

Since PUs are not always transmitting, the probability that a typical PT x_k^p is active based on (1)–(2) is given as $p_a(t)$, where $0 \leq p_a(t) \leq 1$, $\forall t \geq 0$. Similarly, SUs are not always active and the probability that a typical secondary transmitter x_k^s chooses to transmit on channel c_k can be given as $p_b(t)$, where $0 \leq p_b(t) \leq 1$, $\forall t \geq 0$. Although, these probabilities are time-dependent in real life, we assumed that they are time-homogeneous in order not to underestimate interference in both networks while also ensuring simplicity in the modeling. Hence, we considered worst case scenario in which the PU and SU transmit with $p_a(t) = p_b(t) = 1$ and a scenario where $p_a(t) = 0.5$. Rayleigh fading is assumed with $E[h] = 1$, where h is the independent and identically distributed exponential fading coefficient. $l|y_k^*| = ||y_k^*||^{-\alpha}$ represents the large-scale path loss model with path loss exponent α, where $l|y_k^*|$ represents the path loss attenuation between any typical primary or secondary transmitter and its corresponding paired receiver $|y_k^*|$ given that $* = [p, s]$. In order to avoid unnecessary repetition, the basics of stochastic geometry are not presented. These have been presented in earlier works [34]–[36].

2.1 Primary User Interference Control

Under PU interference control mechanism, interference control at the secondary network is ignored and the distributions of active SUs are characterized following PHP. Next, we derive expressions for the PU coverage probability under this mechanism.

2.1.1 Primary User Coverage Probability

Coverage is achieved if the received SINR is greater than a predefined threshold [11], [25], [37]. In such case, the PU transmitted signal is said to be correctly decoded by the intended primary receiver in the presence of interference and noise [11]. Hence, PU coverage probability can be expressed as the probability that the received SINR is greater than the predefined PU SINR threshold i.e. $P(SINR > \theta_p)$.

$$P_{cov}^{p} = P\Big(\frac{P_p h_X l|y_k^p|}{W + I_{pp} + I_{sp}} > \theta_p\Big),$$
$$= \exp(-sW)\mathcal{L}_{I_{pp}}(s)\mathcal{L}_{I_{sp}}(s), \quad (7)$$

where W is the thermal noise power known to be independent of other elements of the given model [13], [20] and is typically negligible [5], [14], [21], $\mathcal{L}_{I_{pp}}$ is the Laplace transform (LT) of the interference from other active PUs to the tagged primary receiver and $\mathcal{L}_{I_{sp}}$ is the LT of interference from active SUs. Note that in our case, there is correlation between I_{pp} and I_{sp}. However, such an analysis is not tractable. Hence, we assumed that I_{pp} and I_{sp} are independent. A similar assumption has been made in [22], [23], [38], with the results showing that such approximation does not affect the reliability of the outcome. The derivations of $\mathcal{L}_{I_{pp}}$ and $\mathcal{L}_{I_{sp}}$ are given next.

Lemma 1 – The LT of PU intra-network interference $\mathcal{L}_{I_{pp}}$ under PU interference control is given as

$$\mathcal{L}_{I_{pp}}(s) = \exp\left\{ -\pi \frac{\gamma \lambda_p^1 (sP_p)^{\frac{\gamma}{\pi}}}{\sin(\gamma)} \right\}. \quad (8)$$

Proof – I_{pp} is the interference from PUs outside the tagged PU exclusion region. The derivation is straightforward and is only presented in Appendix A for completeness.

Lemma 2 – The I_{sp} under PU interference control is generated by SUs outside the exclusion regions of active PUs. Its LT can be represented as

$$\mathcal{L}_{I_{sp}}(s) \leq \exp\left\{ -\pi \frac{\gamma \lambda_s (sP_s)^{\frac{\gamma}{\pi}}}{\sin(\gamma)} \right\}$$
$$\exp\left\{ -2\pi\lambda_p^1 \int_R^\infty \Big(1 - \exp(f(v))\Big) v dv \right\}, \quad (9)$$

where $f(v) = \int_{v-R}^{v+R} cos^{-1}\Big(\frac{-R^2+v^2+r^2}{2vr}\Big) \frac{2\lambda_s r}{1+\frac{r^\alpha}{sP_s}} dr$.

Proof – The LT of I_{sp} is obtained by first taking $I_{sp} = \sum_{x_i^s \in \Phi_s \cap \Xi_R^c} P_s h_x ||y_i^p||^{-\alpha}$. Its proof is similar to Theorem 3 [9] and is omitted for brevity.

Theorem 1 – Following the derivations of $\mathcal{L}_{I_{pp}}$ in (8) and $\mathcal{L}_{I_{sp}}$ in (9), the bound expression for the PU coverage probability at $s = \frac{\theta_p}{P_p l|y_k^p|}$ under PU interference control can be derived as

$$P_{cov}^{p} \leq (-sW) \exp\left\{ -\pi \frac{\gamma \lambda_p^1 (sP_p)^{\frac{\gamma}{\pi}}}{\sin(\gamma)} \right\} \times \exp\left\{ -\pi \frac{\gamma \lambda_s (sP_s)^{\frac{\gamma}{\pi}}}{\sin(\gamma)} \right\}$$
$$\exp\left\{ -2\pi\lambda_p^1 \int_R^\infty \Big(1 - \exp(f(v))\Big) v dv \right\}. \quad (10)$$

Because of the complexity involved in the integration, (10) is difficult to solve. Hence, we made some approximation which are validated in Section VI. At $\alpha = 4$, neglecting the complexity of the integral, a careful integration of the last part of (10), showed that

$$\exp\left\{ -2\pi\lambda_p^1 \int_R^\infty \Big(1 - \exp(f(v))\Big) v dv \right\}$$
$$\approx \exp\left\{ -2\pi\lambda_p^1 \int_R^\infty \left(1 - \exp\left(2\lambda_s \left(\frac{r_p^2}{2}\left(\frac{\theta_p P_s}{P_p}\right)^{\frac{1}{2}} \right.\right.\right.\right.$$
$$\left.\left.\left.\left. \left\{ \tan^{-1}\left(\left(\frac{P_p}{\theta_p P_s}\right)^{\frac{1}{2}} \frac{(v+r)^2}{r_p^2}\right) - \tan^{-1}\left(\left(\frac{P_p}{\theta_p P_s}\right)^{\frac{1}{2}} \frac{(v-r)^2}{r_p^2}\right) \right\} \right) \right) \times \left\{ (v+R)\cos^{-1}\left(\frac{2v(v+R)}{2v(v+R)}\right) \right.\right.$$
$$\left.\left. - (v-R)\cos^{-1}\left(\frac{2v(v-R)}{2v(v-R)}\right) \right\} \right) \right) v dv \right\} \approx 1. \quad (11)$$

Hence, the approximate PU coverage probability can be represented as

$$P_{cov}^{p} \approx \exp\left(-W \frac{\theta_p r_p^4}{P_p} \right) \exp\left(\frac{-\pi^2}{2} \lambda_p^1 \sqrt{\theta_p} r_p^2 \right)$$
$$\exp\left(\frac{-\pi^2}{2} \lambda_s \sqrt{\frac{\theta_p P_s}{P_p}} r_p^2 \right). \quad (12)$$

2.1.2 Secondary User Coverage Probability

The SU coverage probability is the probability that a typical transmitted signal from the secondary transmitter is successfully decoded at the intended secondary receiver in the presence of noise and interference. Similar to (7), SU coverage probability is given as $P(SINR > \theta_s)$, where θ_s is the SINR threshold for secondary transmission.

$$P_{cov}^{s} = \exp(-sW)\mathcal{L}_{I_{ss}}(s)\mathcal{L}_{I_{ps}}(s) \quad (13)$$

For completeness, the expressions of $\mathcal{L}_{I_{ss}}$ and $\mathcal{L}_{I_{ps}}$ are given in the following lemmas.

Lemma 3 – The LT of I_{ss} under PU interference control can be expressed as

$$\mathcal{L}_{I_{ss}}(s) = \exp\left\{ -\pi \frac{\gamma \lambda_s^1 (sP_s)^{\frac{\gamma}{\pi}}}{\sin(\gamma)} \right\}. \quad (14)$$

I_{ss} is generated from active secondary transmitters except the tagged secondary transmitter. The derivation of Lemma 3 is similar to derivations of Lemma 1.

Lemma 4 – The I_{ps} under PU interference control is similar to derivations of Lemma 2 and can be expressed as

$$I_{ps} = \sum_{x_i^p \in \Phi_p^1 \cap \Xi_s^c} P_p h_X ||y_i^s||^{-\alpha}.$$

Since there is no protection at the secondary network under PU interference control, the disk centered on any tagged secondary receiver is the same as the radius of the distance r_s between the secondary transmitter and receiver under the bipolar network model. The LT of I_{ps} is thus given as

$$\mathcal{L}_{I_{ps}}(s) = \exp\left\{ -\pi \frac{\gamma \lambda_p^1 (sP_p)^{\frac{\gamma}{\pi}}}{\sin(\gamma)} \right\} \exp\left\{ 2\lambda_p^1 (g(v)) \right\}, \quad (15)$$

where $g(v) = \int_{v-r_s}^{v+r_s} cos^{-1}\Big(\frac{-r_s^2+v^2+r^2}{2vr}\Big) \frac{r}{1+\frac{r^\alpha}{sP_p}} dr$.

Proof – Lemma 4 is obtained following a similar approach as in Lemma 2 and is omitted for the sake brevity.

Theorem 2 – Following the derivations of I_{ss} and I_{ps}, the bound coverage probability for SUs at $s = \frac{\theta_s}{P_s l|y_k^s|}$ under PU interference control can be derived as

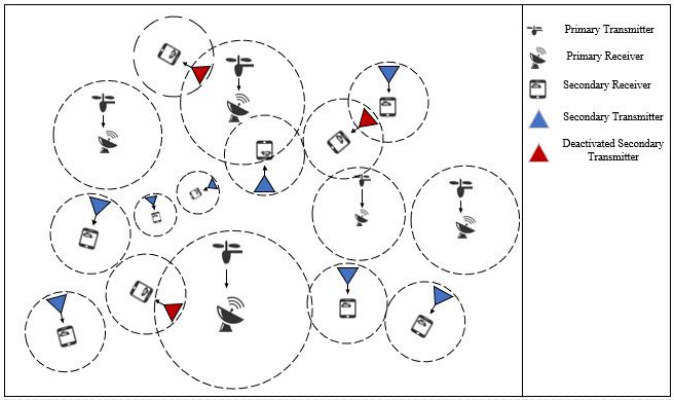

Fig. 2. Users distributions under PU with SU interference control

$$P^{s}_{cov} = (-sW)\exp\left\{-\pi\frac{\gamma\lambda^1_s(sP_s)^{\frac{\gamma}{\pi}}}{\sin(\gamma)}\right\}\times \exp\left\{-\pi\frac{\gamma\lambda^1_p(sP_p)^{\frac{\gamma}{\pi}}}{\sin(\gamma)}\right\}\exp\left\{2\lambda^1_p(g(v))\right\}. \quad (16)$$

At $\alpha = 4$; $\exp\left\{2\lambda^1_p(g(v))\right\} \approx 1$.

Hence, the approximate expression for (16) can be expressed as

$$P^{s}_{cov} \approx \exp\left(-W\frac{\theta_s r_s^4}{P_s}\right)\exp\left(\frac{-\pi^2}{2}\lambda^1_s\sqrt{\theta_s}r_s^2\right) \exp\left(\frac{-\pi^2}{2}\lambda^1_p\sqrt{\frac{\theta_s P_p}{P_s}}r_s^2\right). \quad (17)$$

2.2 Primary with Secondary User Interference Control

In a real system, SUs may not necessarily be close to each other arbitrarily, as observed under primary interference control mechanism, especially if SU QoS is important. Hence, there is a need to protect active SUs from possible interference from other transmitting SUs. Under the primary with secondary user interference control mechanism, interference is controlled at the secondary network in addition to the primary network. In this case, the protection regions of radius $d \geq r_s$ centered on each secondary receiver are also introduced in the secondary network, as shown in Fig. 2. Hence, a typical secondary transmitter must ensure that its location is not within active PUs' exclusion regions and currently active SUs' exclusion regions.

While the distribution of active PUs is not affected by the introduction of protection zones at the secondary network, the distribution of active SUs now follows a mPHP Φ^{11}_s with intensity λ^{11}_s.

2.2.1 Primary user coverage probability under primary with secondary user interference control

In this case, the derivation of the LT of I_{pp} is the same as in Lemma 1 since interference control in the secondary network (as in the case of PU with SU interference control) does not affect distributions of PUs as shown in Fig. 2, while I_{sp} is dominated by interference from SUs outside active PUs and currently active SUs protection regions. The details are provided in the following Lemma.

Lemma 5 – The LT of I_{sp} under PU with SU interference control is given as

$$\mathcal{L}_{I_{sp}}(s) \leq \exp\left\{-\pi\frac{\gamma\lambda_s(sP_s)^{\frac{\gamma}{\pi}}}{\sin(\gamma)}\right\}\times \exp\left\{-2\pi\lambda^1_p\int_R^\infty\Big(1-\exp(f(v))\Big)vdv\right\} \exp\left\{-2\pi\lambda^{11}_s\int_d^\infty\Big(1-\exp(f(w))\Big)wdw\right\}. \quad (18)$$

Proof – The proof is presented in Appendix B.

Theorem 3 – The PU coverage probability under PU with SU interference control at $s = \frac{\theta_p r_p^\alpha}{P_p}$ is given as

$$P^{p}_{cov} \leq (-sW)\exp\left\{-\pi\frac{\gamma\lambda^1_p(sP_p)^{\frac{\gamma}{\pi}}}{\sin(\gamma)}\right\}\exp\left\{-\pi\frac{\gamma\lambda_s(sP_s)^{\frac{\gamma}{\pi}}}{\sin(\gamma)}\right\} \exp\left\{-2\pi\lambda^1_p\int_R^\infty\Big(1-\exp(f(v))\Big)vdv\right\}\times \exp\left\{-2\pi\lambda^{11}_s\int_d^\infty\Big(1-\exp(f(w))\Big)wdw\right\}, \quad (19)$$

where $f(w) = \int_{w-d}^{w+d} cos^{-1}\left(\frac{-d^2+w^2+r^2}{2wr}\right)\frac{2\lambda_s r}{1+\frac{r^\alpha}{sP_s}}dr$.

As in Theorem 1, the presence of integrals in (19) makes it difficult to solve. Hence, we obtained the approximation of Theorem 3 following similar observations as in (11). Hence, the approximation for the bound of Theorem 3 at $\alpha = 4$ is given as

$$P^{p}_{cov} \approx \exp\left(-W\frac{\theta_p r_p^4}{P_p}\right)\exp\left(\frac{-\pi^2}{2}\lambda^1_p\sqrt{\theta_p}r_p^2\right) \exp\left(\frac{-\pi^2}{2}\lambda_s\sqrt{\frac{\theta_p P_s}{P_p}}r_p^2\right). \quad (20)$$

Surprisingly, the approximation obtained is tight bound despite the fact that some part of (19) was neglected as will be shown in Section VI, demonstrating the reliability of the approximation approach.

2.2.2 Secondary user coverage probability under primary with secondary user interference control

The derivation of SU coverage probability under PU with SU interference control is not straightforward. Note that the interference I_{ss} is dominated by interference from the SU of intensity λ^1_s outside the tagged SU protection region, the LT of I_{ss} can be given as

$$\mathcal{L}_{I_{ss}} = \exp\left\{-2\pi\lambda^1_s\int_d^\infty\frac{r}{1+\frac{r^\alpha}{sP_s}}dr\right\}. \quad (21)$$

The $\mathcal{L}_{I_{ps}}$ however, can be obtained from

$$I_{ps} = \sum_{x^p_i\in\Phi^1_p\cap b^c(y,d)} P_p h_X||y^s_i||^{-\alpha},$$

since the disk centered on the tagged SU is the same as the radius of the SU protection region. The derivation of $\mathcal{L}_{I_{ps}}$ follows the same process as in Appendix B. The SU coverage probability under this mechanism is given in Theorem 4.

Theorem 4 – The SU coverage probability under PU with SU interference control at $s = \frac{\theta_s r_s^{\alpha}}{P_s}$ is given as

$$P_{cov}^{s} = (-sW)\exp\left\{ -\pi\frac{\gamma\lambda_p^1(sP_p)^{\frac{\gamma}{\pi}}}{\sin(\gamma)}\right\}$$
$$\exp\left\{ -2\pi\lambda_s\exp(-\lambda_p\pi R^2)\int_d^{\infty}\frac{r}{1+\frac{r^{\alpha}}{sP_s}}dr\right\}$$
$$\exp\left\{2\lambda_p^1(g(z))\right\}, \quad (22)$$

where $g(z) = \int_{v-d}^{v+d} cos^{-1}\left(\frac{-d^2+v^2+r^2}{2vr}\right)\frac{r}{1+\frac{r^{\alpha}}{sP_p}}dr$. At $\alpha = 4$, the approximate expression of Theorem 4 is given as

$$P_{cov}^{s} \approx \exp\left(-W\frac{\theta_s r_s^4}{P_s}\right)\exp\left(-\lambda_s^1\left\{\frac{\pi^2}{2}r_s^2\sqrt{\theta_s}\right.\right.$$
$$\left.\left. -\pi\frac{\tan^{-1}\left(\frac{d^2}{\sqrt{\theta_s}r_s^2}\right)}{\frac{1}{\sqrt{\theta_s}r_s^2}}\right\}\right)\exp\left(\frac{-\pi^2}{2}\lambda_p^1\sqrt{\frac{\theta_s P_p}{P_s}}r_s^2\right) \quad (23)$$

The tightness of this approximate expression will also be demonstrated in Section VI.

2.3 Applications in Non-orthogonal multiple access

Integration of NOMA techniques into CRN has the possibility to further improve spectral efficiency and system capacity while also enhancing massive connectivity. With NOMA techniques, multiple users are allowed to simultaneously access the network at the same time and frequency through the use of non-orthogonal resources such as different power levels or low-density spreading codes. SUs can take this opportunity to cooperate with PUs on PUs assigned channels, improving spectrum access opportunity in the proces. NOMA, however, results in more severe interference in the network when compared with conventional OMA [39].

In order to further improve spectral efficiency using NOMA technique, SUs can be allowed to be active inside PUs exclusion zones provided that the maximum permissible interference power constraint at the tagged PR is satisfied. Hence, the QoS required at the typical PR y_k^p located within the coverage of its corresponding PT x_k^p is given as

$$P\left(\frac{P_p|h_X|^2}{W+\sum_{x_i^p\in\Phi_p^I\setminus x_k^p}P_p|h_X|^2+\sum_{x_i^s\in\Phi_s^{II}}P_s|h_x|^2+b_o}\geq\theta_p\right), \quad (24)$$

where $b_o = \sum_{x_{i,R}^s\in\Phi_s}P_s|h_x|^2$ is the aggregate interference from active STs within the protection region R of the tagged PT x_k^p, $|h_X|^2$ is the channel gain between the PT and PR, and $|h_x|^2$ is the channel gain between the STs and PR. To satisfy the interference constraints at the PR, the transmit power of STs located within any PU exclusion zone in a NOMA based CRN can be constrained to

$$P_s^{NOMA} \leq \min\left\{\left(\frac{I_p}{\max_{y_k^p\in\Phi_p^{II}}|h_x|^2}\right), P_s\right\}, \quad (25)$$

where $P_s^{NOMA} = \sum_i^{n_s,R}P_s$ signifies the overall power of all SUs within the considered PU's exclusion zone, and I_p is the maximum permissible interference power at the tagged PR.

In order to satisfy the QoS requirement at the secondary receivers, successive interference cancellation technique is one of the most efficient methods. Interference at a typical SR is obtained from STs and PT of higher gain while STs and PT with lower gain are removed using interference cancellation technique [40]. At a typical secondary receiver (SR) y_k^s located within the coverage of an active PT x_k^p, the QoS ($SINR_{y_k^s}\geq\theta_s$) at the SR is obtained as

$$P\left(\frac{P_s|h_y|^2}{W+\sum_{x_i^s\in\Phi_s\setminus x_k^s\setminus b_o}P_s|h_y|^2+\sum_{x_i^p\in\Phi_s^{II}\setminus x_k^p}P_p|h_Y|^2}\geq\theta_s\right), \quad (26)$$

where $|h_y|^2$ is the channel gain between the ST and SR, and $|h_Y|^2$ is the channel gain between PTs and SR.

Asides implementation complexity involved in NOMA based CRN, high performance spectrum sensing is required to practically differentiate between PTs and STs, since the performance analysis of the received signal based on the popular independence assumption in conventional OMA is invalid in this case [39]. NOMA based CRN is, hence, the subject of future research.

3 Optimization of the number of simultaneous active users supported

Asides coverage probability, the number of simultaneous active users supported is another important metrics when investigating the performance of interference mechanisms in CRN. The number of simultaneous active users supported depicts the density of SUs that can be active under a given radius of protection regions. A minimal difference between SU baseline intensity and the number of simultaneous active users supported means PU spectrum holes are being used effectively by the SUs, signifying effective usage of the spectrum in the process. Since it is necessary to guarantee successful communication between two communicating pairs in the network, the relationship between these two metrics is intuitively an inverse one. A high desired threshold for coverage probability then means less number of simultaneous active users can be supported, while a lower coverage threshold increases the possibility of an outage in the network, though with an increase in the number of simultaneous active users supported. Finding a trade-off between these two parameters therefore becomes imperative.

3.1 Number of simultaneous active users supported under PU Interference Control Mechanism

The number of simultaneous active users supported, in this case, is given as $S_E = \lambda_s\exp(-\lambda_p\pi R^2)$. Note that the number of simultaneous active users supported depends on the radius of the PU protection region, which is proportional to the PU coverage probability. Also, an increase in R means less spaces are available for secondary transmissions. The

objective will therefore be to select R at which the number of simultaneous active users supported is maximal. Due to their dependence on R, we can express the PU coverage probability given in (10) and SU coverage probability given in (16) in the form of $P^p_{cov}(S_E, R) > 0$ and $P^s_{cov}(S_E, R) > 0$ respectively. Hence, the optimization problem can be derived as follows:

$$\max_{\lambda_s \geq S_E \geq 0, R_{max} \geq R \geq r_p + r_s} S_E = \lambda_s \exp(-\lambda_p \pi R^2).$$

Subject to

$$P^p_{cov}(S_E, R) > 0$$

$$P^s_{cov}(S_E, R) > 0$$

In order to limit inter-network interference, the minimum radius of R should not be less than the sum of maximum distance between PU transmitter-receiver pair r_p and SU transmitter-receiver pair r_s. Hence, $r_p + r_s$ was taken as the minimum R as in [17] so as to ensure a definite distance between primary transmitters and secondary receivers, while at R_{max}, a typical PU signal can no longer be detected by the secondary transmitters. Similarly, we know that the maximum number of SUs that can be active simultaneously cannot be greater than λ_s. To ensure that the problem is feasible, $P^p_{cov}(0, R) > 0$ and $P^s_{cov}(0, R) > 0$ are assumed to be satisfied $\forall_R \in [r_p + r_s, R_{max}]$. Therefore, the smallest upper bound $M(R) \geq 0$ for S_E, such that $S_E \in [0, M(R)]$ satisfies $P^p_{cov}(S_E, R) > 0$ and $P^s_{cov}(S_E, R) > 0$, while $S_E > M(R)$ violates at least one of these constraints or the implicit constraint $S_E \in [0, \lambda_s]$ can be given as

$$M(R) = min\Bigg[\exp(-\lambda_p \pi R^2) \left\{ \frac{-ln(P^p_{cov}) + \frac{W\theta_p r_p^4}{P_p} + \left(\frac{-\pi^2}{2} \lambda_p^1 \sqrt{\theta_p} r_p^2 \right)}{\left(\frac{-\pi^2}{2} \sqrt{\frac{\theta_p P_s}{P_p}} r_p^2 \right)} \right\}, \frac{-ln(P^s_{cov}) + \left(-W \frac{\theta_s r_s^4}{P_s} \right) + \left(\frac{-\pi^2}{2} \lambda_p^1 \sqrt{\frac{\theta_s P_p}{P_s}} r_s^2 \right)}{\left(\frac{-\pi^2}{2} \sqrt{\theta_s} r_s^2 \right)}, \lambda_s^1 \Bigg]. \tag{27}$$

Equation (27) is obtained by deriving S_E from (12) and (17). Hence the optimal point can be found at the points $(M(R), R), \forall_R \in [r_p + r_s, R_{max}]$. The same conclusion was reached for similar problems in [17].

3.2 Number of simultaneous active users supported under PU with SU Interference Control Mechanism

The number of simultaneous active users supported under PU with SU interference control mechanism can be expressed as

$$S_E = \lambda_s \exp(-\pi(\lambda_p R^2 + \lambda_s d^2)).$$

Here, PU and SU coverage probabilities as well as the number of simultaneous active users supported depend on both SU protection region d and PU protection region R. Finding the trade-off between these two parameters will be useful towards effective and efficient channel usage. Similarly, due to their dependence on R and d, the PU coverage probability given in (19) and the SU coverage probability given in (22) can be expressed in the form of $P^p_{cov}(d, R) > 0$ and $P^s_{cov}(d, R) > 0$ respectively. The optimization problem, in this case, can be formulated as

$$\max_{d_{max} \geq d \geq 0, R_{max} \geq R \geq r_p + r_s} S_E = \lambda_s \exp(-\pi(\lambda_p R^2 + \lambda_s d^2))$$

subject to

$$P^p_{cov}(d, R) > 0$$

$$P^s_{cov}(d, R) > 0.$$

In order to ensure a feasible problem for all R, $\forall_R \in [r_p + r_s, R_{max}]$, we assumed that $P^p_{cov}(d_{max}, R) > 0$ and $P^s_{cov}(d_{max}, R) > 0$, such that a large d will satisfy the given constraints. A lower bound $m(R) \leq R_{max}$ hence, exists on d such that $d \in [m(R), d_{max}]$ satisfies $P^p_{cov}(d, R) > 0$ and $P^s_{cov}(d, R) > 0$, while $d < m(R)$ violates at least one of the constraints or the implicit constraint $d \in [0, d_{max}]$. The optimal point can be found at the points $(m(R), R)$, $\forall_R \in [r_p + r_s, R_{max}]$. The closed form expression for $m(R)$, however, does not exist. Hence, we simply adjusted the optimization problem with the objective of selecting R at which the S_E is maximal since interference reduction at any typical PU is non-negotiable; the optimization problem can be re-formulated as

$$\max_{\lambda_s \geq S_E \geq 0, R_{max} \geq R \geq r_p + r_s} S_E = \lambda_s \exp(-\pi(\lambda_p R^2 + \lambda_s d^2))$$

subject to

$$P^p_{cov}(S_E, R) > 0$$

$$P^s_{cov}(S_E, R) > 0.$$

This optimization problem is similar to the one given under PU interference control mechanism. From the approximation presented in (20) and (23), the smallest upper bound $M(R) \geq 0$ for S_E can be given as

$$M(R) = min\Bigg[\exp(-\pi(\lambda_p R^2 + \lambda_s d^2)) \left\{ \frac{-ln(P^p_{cov}) + \frac{W\theta_p r_p^4}{P_p} + \left(\frac{-\pi^2}{2} \lambda_p^1 \sqrt{\theta_p} r_p^2 \right)}{\left(\frac{-\pi^2}{2} \sqrt{\frac{\theta_p P_s}{P_p}} r_p^2 \right)} \right\}, \exp(-\lambda_p \pi d^2) \frac{-ln(P^s_{cov}) + \left(-W \frac{\theta_s r_s^4}{P_s} \right) + \left(\frac{-\pi^2}{2} \lambda_p^1 \sqrt{\frac{\theta_s P_p}{P_s}} r_s^2 \right)}{\frac{\pi^2}{2} \sqrt{\theta_s} r_s^2 - \pi \frac{\tan^{-1}\left(\frac{d^2}{\sqrt{\theta_s} r_s^2} \right)}{\frac{1}{\sqrt{\theta_s} r_s^2}}}, \lambda_s^1 \Bigg]. \tag{28}$$

4 ANALYZING THE EFFECTS OF BIPOLAR NETWORK MODEL

Relaxing the bipolar network model assumption means that the distance r_p between any typical primary transmitter and its corresponding primary receiver follows a random distribution. Similarly, at the secondary network, the distance r_s separating a typical secondary transmitter and its corresponding secondary receiver is randomized. This approach has been clearly presented and demonstrated in a heterogeneous cellular network [22], [23], making the adoption of such an interesting approach in this work quite easy and straightforward. In this case, the radius of protection zones for both networks no longer directly depend on the fixed transmitter-receiver pair distance as in the case of the bipolar network model.

Relaxing the bipolar network model assumption under PU interference control, we considered a case in which the distance between a typical primary transmitter and its corresponding receiver cannot be greater than v_p. Hence, the radius of the PU protection zone centered at the typical primary receiver located at the origin is given as $R \geq v_p$. A typical primary transmitter is then assumed to be uniformly located in the disk of radius R centered at its corresponding receiver. The radius r_p therefore follows $f_{r_p}(l) = \frac{2l}{R^2} 1_{l \leq R}$. The inter-network dependency between the primary and secondary network means the distribution of radius r_s can be approximated as a Weibull distribution [41], which can be expressed as

$$f_{r_p}(l) = \begin{cases} \frac{k}{\lambda}\left(\frac{l}{\lambda}\right)^{k-1} \exp(\frac{-l}{\lambda})^k & l \geq 0 \\ 0 & l < 0, \end{cases} \tag{29}$$

where the parameter $k > 0$ and $\lambda > 0$ represent the shape and scale parameter of the Weibull distribution respectively.

The approximate PU coverage probability taken at $s = \frac{\theta_p}{(P_p l^{-\alpha})}$ can be expressed as

$$P^p_{cov} = \int_0^R \exp(-sW)\mathcal{L}_{I_{pp}}(s)\mathcal{L}_{I_{sp}}(s)\frac{2l}{R^2}dl. \tag{30}$$

Also, the approximate SU coverage probability taken at $z = \frac{\theta_s}{P_s l^{-\alpha}}$ can be expressed as

$$P^s_{cov} = \int_0^\infty \exp(-zW)\mathcal{L}_{I_{pp}}(z)\mathcal{L}_{I_{sp}}(z)\frac{k}{\lambda}\left(\frac{l}{\lambda}\right)^{k-1} \exp(\frac{-l}{\lambda})^k dl. \tag{31}$$

Similarly, under the PU with SU interference control mechanism, a typical primary transmitter can be assumed to be uniformly distributed in the disk of radius R centered at its corresponding primary receiver. Hence the PU coverage probability is the same as in the previous case. For the secondary network, the distribution of the secondary transmitter centered on its corresponding secondary receiver is hard to derive. This is because secondary transmitters are not allowed to be active inside the primary exclusion zone. Since our derivation under the bipolar network model assumption prevents secondary transmitters inside primary zones, we assume that a tagged secondary transmitter is also uniformly distributed around its corresponding receiver. Hence, the SU coverage probability can be expressed as

$$P^s_{cov} = \int_0^d \exp(-zW)\mathcal{L}_{I_{ss}}(z)\mathcal{L}_{I_{ps}}(z)\frac{2l}{d^2}dl. \tag{32}$$

The tightness of these expressions will be shown in Section VI of this paper.

5 INTERFERENCE MODEL IN COGNITIVE RADIO NETWORK UNDER INDEPENDENCE DISTRIBUTION ASSUMPTION

For the sake of comparison, PHP and the modified version of PHP in Section II were obtained after independent thinning of HPPP. Under this assumption, the closed-form expressions obtained are more analytically tractable in relation to the PHP and modified version of PHP presented in Section II, though coverage is slightly overestimated, as will be seen in the next section. PU and SU coverage probabilities under this assumption are presented in the following propositions.

Proposition 1 – The PU coverage probability under the PU interference control mechanism with the assumption of independence among active PUs and SUs can be expressed as

$$P^p_{cov} = (-sW)\exp\left\{-\pi\frac{\gamma\lambda_p(sP_p)^{\frac{\gamma}{\pi}}}{\sin(\gamma)}\right\} \exp\left(-2\pi\lambda^1_s\int_R^\infty \frac{r}{1+\frac{r^\alpha}{sP_s}}dr\right). \tag{33}$$

Proof – I_{pp} is derived based on the assumption that active PUs follow HPPP. Hence,

$$I_{pp} = \sum_{x^p_i \in \Phi_p \setminus x^p_k} P_p h_X ||y^p_i||^{-\alpha}.$$

I_{sp}, on the other hand, is derived based on the assumption that SUs are distributed following PHP obtained after an independent thinning of PPP. SUs inside active PUs' protection zones are assumed to be automatically deactivated.

Proposition 2 – The SU coverage probability under the PU interference control mechanism with the assumption of independence among active PUs and SUs can be expressed as

$$P^s_{cov} = (-zW)\exp\left\{-\pi\frac{\gamma\lambda^1_s(zP_s)^{\frac{\gamma}{\pi}}}{\sin(\gamma)}\right\} \exp\left(-2\pi\lambda^1_p\int_0^\infty \frac{r}{1+\frac{r^\alpha}{zP_p}}dr.\right) \tag{34}$$

Proof – Since SUs are assumed to be inactive inside PUs' protection zones, I_{ss} is obtained by approximating the distribution of SUs as a PPP while for I_{ps}, the lower bound of the integral was chosen since a typical SU is not protected under PU interference control.

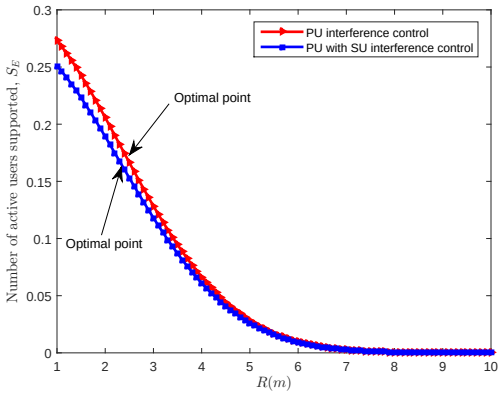

Fig. 3. Optimized number of simultaneous active users supported. $P_{cov}^p = P_{cov}^s = 0.8$, $D = 0.2991$.

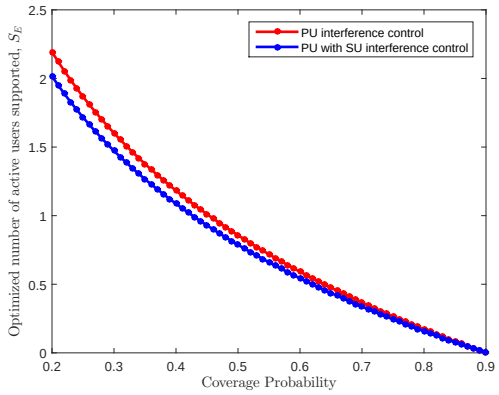

Fig. 4. The relationship between the two metrics of interests.

Proposition 3 – The PU coverage probability under the PU with SU interference control mechanism with the assumption of independence among active PUs and SUs can be expressed as

$$P_{cov}^p = (-sW)\exp\left\{-\pi\frac{\gamma\lambda_p(sP_p)^{\frac{\gamma}{\pi}}}{\sin(\gamma)}\right\} \exp\left(-2\pi\lambda_s^1\exp(-\lambda_s\pi d^2)\int_R^\infty \frac{r}{1+\frac{r^\alpha}{sP_s}}dr\right). \quad (35)$$

Under this scenario, I_{sp} is obtained from active SUs outside the tagged PU protection region R. I_{pp} is the same as in Proposition 1.

Proposition 4 – The SU coverage probability under the PU and SU interference control mechanism with the assumption of independence among active PUs and SUs can be expressed as

$$P_{cov}^s = (-zW)\exp\left(-2\pi\lambda_s^1\exp(-\lambda_s\pi d^2\int_d^\infty \frac{r}{1+\frac{r^\alpha}{zP_s}}dr\right) \exp\left(-2\pi\lambda_p\int_d^\infty \frac{r}{1+\frac{r^\alpha}{zP_p}}dr\right). \quad (36)$$

I_{ss} is obtained from active SUs outside the tagged SU protection region and the I_{ps} is generated from PUs expected to be outside the tagged SU protection region.

6 NUMERICAL SIMULATIONS

We now carry out numerical simulations of the approaches presented in the previous sections to demonstrate the tightness and accuracy of the expressions. Unless otherwise stated, the following numerical values were used in simulations: $\lambda_s = 0.3$, $\lambda_p = 0.03$, $\theta_p = \theta_s = 10$, $r_p = 0.5$, $r_s = 0.1$, $P_p = 1$, $P_s = 0.025$, $\alpha = 4$, $\zeta = 81$, and $W = 10^{-5}$. The optimal point of R at which S_E reaches its maximum under the defined parameters is shown in Fig. 3. Under PU with SU interference control, a slightly smaller S_E indicates that the introduction of protection in the secondary network further reduces the number of simultaneous active users supported. Also, a smaller R is

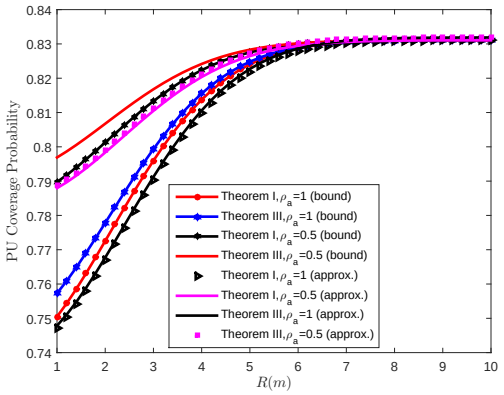

Fig. 5. PU coverage probability

required to achieve the desired coverage, since interference from SUs is reduced by interference control in the secondary network. The relationship between the optimized S_E and coverage probability is presented in Fig. 4, confirming the inverse relationship between the two metrics.

Because of the tight closeness between various PU parameters, we first present the relationship between the bound expressions in Theorem 1 and 3 and their corresponding approximations at $p_a = 0.5$ and $p_a = 1$ in Fig. 5. The slightly loose bound between the approximations and the bounds suggests that interference in the primary network is dominated by interference from active SUs that were thinned out during approximation. Similarly, Theorem 2 and Theorem 4 with their corresponding approximations are presented in Fig. 6. The tightness observed between the bounds and approximate expressions shows the reliability of the theoretical analysis used in approximating the PHP and the modified PHP. Higher coverages were obtained at $p_a = 0.5$ owing to reduced PUs activities, leading to reduced intra-network interference in the primary network and reduced interference from the primary network in the secondary network. When interference is also controlled at the secondary network, an increase in PU and SU coverage probabilities signifies the effects of SU activities on coverage. We have considered the worst-case scenario of $p_b = 1$ to avoid coverage overestimation. Both PU and SU coverage

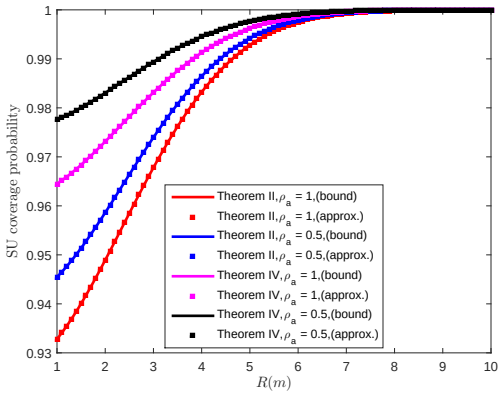

Fig. 6. SU coverage probability.

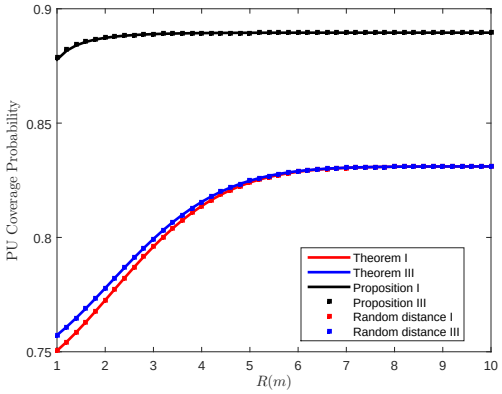

Fig. 7. PU coverage probability under random and independence assumption.

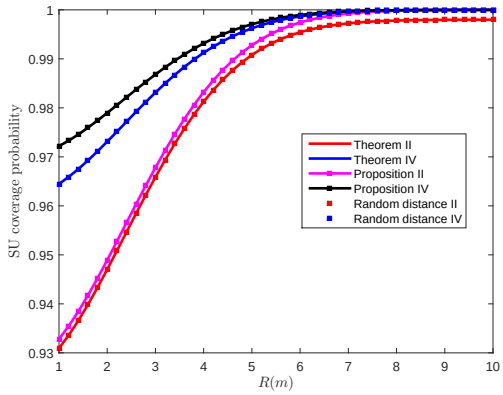

Fig. 8. SU coverage probability under random and independence assumption

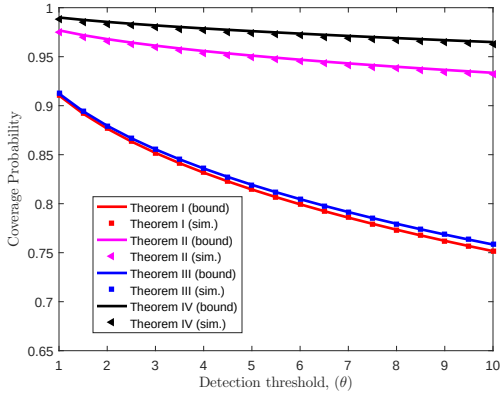

Fig. 9. PU and SU coverage probabilities.

probabilities are expected to increase at $p_b < 1$.

The analysis of the effects of the bipolar network model assumption shows that randomizing the distance between the transmitting pairs does not affect the performance of the network under the selected assumptions. This is presented in Fig. 7 and Fig. 8 for the primary and secondary network respectively. The outcome shows that there is a tight closeness under PU interference control and PU with SU interference control when the bipolar network model assumption is relaxed. The case of independence distributions, however, shows that coverage is overestimated when independence is assumed among users. In all cases, PU and SU coverage probabilities are observed to increase with the PU protection region radius to the point R_{max} where activities of others users do not have an effect on the coverage of the tagged user under the worst-case scenario where $p_a = p_b = 1$. PU and SU coverage probabilities presented in Fig. 9 decrease with an increase in SINR threshold, as expected.

Fig. 10 and Fig. 11 show the relationship between PU and SU coverage probabilities with SU transmit power respectively. As expected, SU coverage probability increases with an increase in SU transmit power at a constant SINR threshold for secondary transmission. Conversely, PU coverage probability decreases with an increase in SU transmit power at a constant SINR threshold for PU transmission. This is unsurprising because interference from the secondary network in the primary network is expected to increase with an increase in SU transmit power. Hence low SU transmit power with other parameters constant will increase PU coverage. While SU transmission power is proportional to SU coverage, it is inversely proportional to the number of simultaneous active users that can be supported.

Stochastic characterization of interference in wireless networks is usually carried out with the aim of achieving tractable analysis, while still obtaining accurate results. Hence, most of the existing efforts [5], [17], [22], [23], etc. usually resort to various simplifications and assumptions, which can lead to underestimation of interference in primary and secondary networks as shown in Fig. 12 and Fig. 13 respectively. In the proposed analyses, we relaxed some of these assumptions and simplifications as presented in the previous Sections. We believe that our analyses are likewise tractable.

7 Conclusion

One of the benefits of CRN is its capability to allow effective and efficient use of spectral resources, which are needed to ensure continuous evolution in wireless technology. With this important benefit, unlicensed users can make use of licensed bands without disrupting the activities of the PUs. In order to ensure this, interference control and management

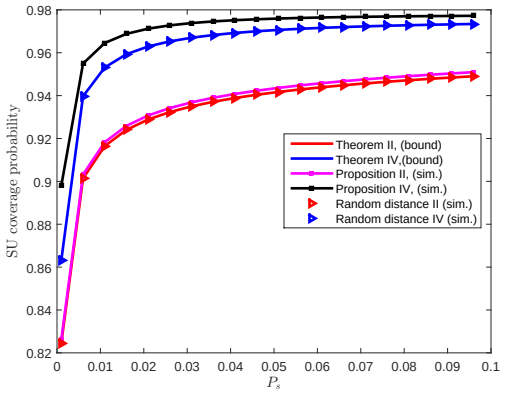

Fig. 10. Effects of P_s on SU coverage probability

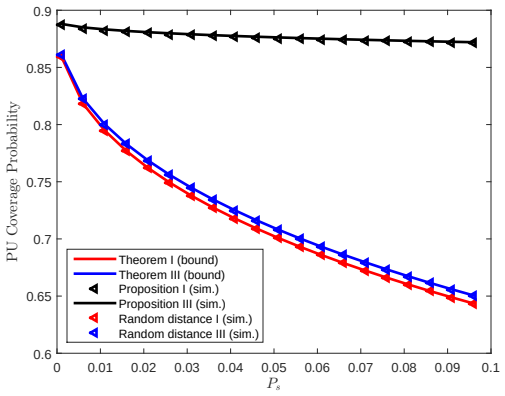

Fig. 11. Effects of P_s on PU coverage probability

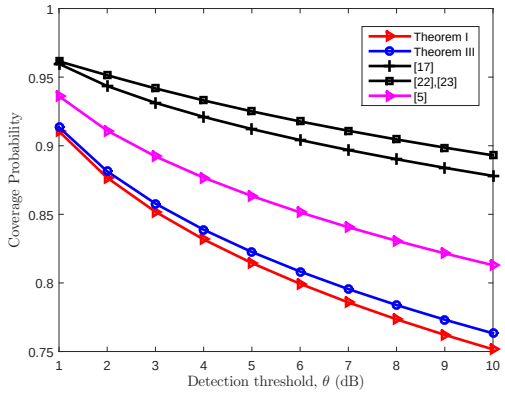

Fig. 12. Performance of the proposed analysis in primary network.

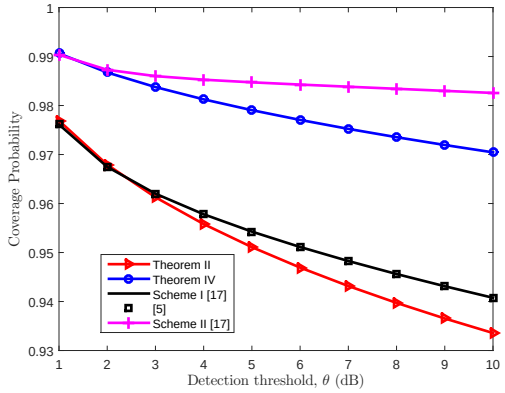

Fig. 13. Performance of the proposed analysis in secondary network.

remain an important requirement in the network. We have presented interference control and management using SG in CRN, in which locations of SUs are not independent of the locations of PUs. Two control mechanisms were considered. Under PU interference control, the distributions of active SUs follow PHP, while the location of SU under PU with SU interference control follows a modified version of PHP.

We also relaxed some of the commonly made assumptions in order to analyze their effects on the performance of CRN. The outcome of numerical simulations shows that bipolar network model assumption is useful while, commonly made independence assumption was found to overestimate coverage in the network, though produces more tractable analysis. In future, we will consider introduction of queuing theory so as to understand the effects of waiting that results when a secondary transmitter is not allowed to transmit because of channels constraints, making it necessary for such transmitter to wait for an appropriate time until there is an idle channel suitable for its transmission. Understanding the effects of such waiting period on SUs QoS will be interesting.

ACKNOWLEDGMENTS

The authors will like to acknowledge Dr. Hesham ElSawy of King Fahd University of Petroleum and Minerals Saudi Arabia, for his valuable suggestions and comments to this work.This work was supported by the SENTECH Chair in Broadband Wireless Multimedia Communications (BWMC), Department of Electrical, Electronics and Computer Engineering, University of Pretoria, South Africa.

REFERENCES

[1] S. Lee, R. Zhang, and K. Huang, "Opportunistic wireless energy harvesting in cognitive radio networks", *IEEE Transactions on Wireless Communications*, vol. 12, no. 9, pp. 4788–4799, Sep. 2013.

[2] X. Song, C. Yin, D. Liu, and R. Zhang, "Spatial throughput characterization in cognitive radio networks with threshold-based opportunistic spectrum access", *IEEE Journal on Selected Areas in Communications*, vol. 32, no. 11, pp. 2190–2204, Nov. 2014.

[3] X. Song, C. Yin, D. Liu, and R. Zhang, "Spatial opportunity in cognitive radio networks with threshold-based opportunistic spectrum access", *in IEEE International Conference on Communications (ICC)*, Budapest, June, 2013, pp. 2695–2700.

[4] S. Lee, and G. Hwang, "A new analytical model for optimized cognitive radio networks based on stochastic geometry", *Journal of Industrial and Management Optimization*, vol. 13, no. 4, pp. 1883–1899, April 2017.

[5] C. Lee, and M. Haenggi, "Interference and outage in Poisson cognitive networks", *IEEE Transactions on Wireless Communications*, vol. 11, no. 4, pp. 1392–1401, April 2012.

[6] J. Kim, S. W. Ko, H. Cha, S. Kim, and S. L. Kim, "Sense-and-predict: Harnessing spatial interference correlation for opportunistic access in cognitive radio networks" [Online], Feb. 2014, Available: *arXiv preprint arXiv: 1802.01088*.

[7] C. Zhai, H. Chen, X. Wang, X., and J. Liu, "Opportunistic spectrum sharing with wireless energy transfer in stochastic networks", *IEEE Transactions on Communications*, vol. 66, no. 3, pp. 1296–1308, Mar. 2018.

[8] S. Kusaladharma, P. Herath, and C. Tellambura, "Underlay interference analysis of power control and receiver association schemes", *IEEE Transactions on Vehicular Technology*, vol. 65, no. 11, pp. 8978–8991, Nov. 2016.

[9] Z. Yazdanshenasan, H. Dhillon, M. Afshang, and P. Chong, "Poisson hole process: Theory and applications to wireless networks", *IEEE Transactions on Wireless Communications*, vol. 15, no. 11, pp. 7531–7546, Nov. 2016.

[10] J. Oh, and W. Choi, "A hybrid cognitive radio system: A combination of underlay and overlay approaches", *in IEEE Vehicular Technology Conference Fall (VTC 2010-Fall)*, Ottawa, Sept. 2010, pp. 1–5.

[11] S. Sabuj, and M. Hamamura, "Uplink modeling of cognitive radio network using stochastic geometry", *Performance Evaluation*, vol. 117, pp. 1–15, Dec. 2017.

[12] A. Sakr, and E. Hossain, "Cognitive and energy harvesting-based D2D communication in cellular networks: Stochastic geometry modeling and analysis", *IEEE Transactions on Communications*, vol. 63, no. 5, pp. 1867–1880, May 2015.

[13] T. Nguyen, and F. Baccelli, "A stochastic geometry model for cognitive radio networks", *The Computer Journal*, vol. 55, no. 5, pp. 534–552, May 2012.

[14] M. Haenggi, J. Andrews, F. Baccelli, O. Dousse, and M. Franceschetti, "Stochastic geometry and random graphs for the analysis and design of wireless networks", *IEEE Journal on Selected Areas in Communications*, vol. 27, no. 7, pp. 1029–1046, Sept. 2009.

[15] H. ElSawy, E. Hossain, and M. Haenggi, "Stochastic geometry for modeling, analysis, and design of multi-tier and cognitive cellular wireless networks: A survey", *IEEE Communications Surveys and Tutorials*, vol. 15, no. 3, pp. 996–1019, July 2013.

[16] H. ElSawy, A. Sultan-Salem, M. Alouini, and M. Win, "Modeling and analysis of cellular networks using stochastic geometry: A tutorial", *IEEE Communications Surveys and Tutorials*, vol. 19, no. 1, pp.167–203, Jan. 2017.

[17] U. Tefek and T. Lim, "Interference management through exclusion zones in two-tier cognitive networks", *IEEE Transactions on Wireless Communications*, vol. 15, no. 3, pp. 2292–2302, Mar. 2016.

[18] A. Busson, B. Jabbari, A. Babaei, and V. Vèque, "Interference and throughput in spectrum sensing cognitive radio networks using point processes", *Journal of Communications and Networks*, vol. 16, no. 1, pp. 67–80, Feb. 2014.

[19] C. Rattaro, P. Bermolen, F. Larroca, and P. Belzarena, "A Stochastic Geometry Analysis of Multichannel Cognitive Radio Networks", *in Proceedings of the 9th Latin America Networking Conference*, Valparaiso, Oct. 2016, pp. 32–38.

[20] T. Nguyen, and F. Baccelli, "A probabilistic model of carrier sensing based cognitive radio", *in IEEE New Frontiers in Dynamic Spectrum*, Singapore, April 2010, pp. 1–12.

[21] X. Song, X. Meng, X. Shen, and C. Jia, "Cognitive radio networks with primary receiver assisted interference avoidance protocol", *IEEE Access*, vol. 6, pp. 1224–1235, Feb. 2018.

[22] N. Deng, W. Zhou, and M. Haenggi, "A heterogeneous cellular network model with inter-tier dependence", *in IEEE Global Communications Conference (GLOBECOM)*, Austin, Dec. 2014, pp. 1522–1527.

[23] N. Deng, W. Zhou, and M. Haenggi, "Heterogeneous cellular network models with dependence", *IEEE Journal on Selected Areas in Communications*, vol. 33, no. 10, Oct. 2015, pp. 2167–2181.

[24] I. Flint, H. Kong, N. Privault, P. Wang, and D. Niyato, "Analysis of heterogeneous wireless networks using Poisson hard core hole process", *IEEE Transactions on Wireless Communications*, vol. 16, no. 11, pp. 7152–7167, Nov. 2017.

[25] Z. Yazdanshenasan, H. Dhillon, M. Afshang, and P. Chong, "Tight bounds on the Laplace transform of interference in a Poisson hole process", *In IEEE Communications (ICC)*, Malaysia, May 2016, pp. 1–6.

[26] M. Afshang, and H. Dhillon, "Spatial modeling of device-to-device networks: Poisson cluster process meets Poisson hole process", *In IEEE Signals, Systems and Computers*, Pacific Grove, Nov. 2015, pp. 317–321.

[27] A. Oluwaranti, and S. Okegbile, "Two state Markov chain based predictive model for cognitive radio spectrum availability: a conceptual approach", in IEEE Future Technologies Conference (FTC), San Francisco, Dec. 2016, pp. 179–186.

[28] M. M. Deshmukh, S. M. Zafaruddin, A. Mihovska, and R. Prasad, "Stochastic-Geometry Based Characterization of Aggregate Interference in TVWS Cognitive Radio Networks," IEEE Systems Journal, vol. 13, no. 3, pp. 2728-2731, April 2019.

[29] L. Irio, R. Oliveira, and D. B. da Costa, "Highly Accurate Approaches for the Interference Modeling in Coexisting Wireless Networks," IEEE Communications Letters, vol. 23, no. 9, pp. 1652-1656, Jun. 2019.

[30] Y. Yang, L. Dai, J. Li, S. Mumtaz, and J. Rodriguez, "Optimal spectrum access and power control of secondary users in cognitive radio networks," EURASIP Journal on Wireless Communications and Networking, vol. 2017, issue 1, pp. 98, Dec. 2017.

[31] B. Gu, C. Zhang, H. Wang, Y. Yao, and X. Tan, "Power control for cognitive M2M communications underlaying cellular with fairness concerns," IEEE Access, vol. 7, pp. 80789-80799, April 2019.

[32] M. Zhou, X. Zhao, and H. Yin, "A robust energy-efficient power control algorithm for cognitive radio networks," Wireless Networks, vol. 25, no. 4, pp. 1805-1814, May 2019.

[33] J. Hu, G. Li, D. Bian, L. Gou, and C. Wang, "Optimal Power Control for Cognitive LEO Constellation with Terrestrial Networks," IEEE Communications Letters, Dec. 2019.

[34] M. Haenggi, and R. Ganti, "Interference in large wireless networks", *NOW Foundations and Trends in Networking*, vol. 3, no. 2, Nov. 2009, pp. 127–248.

[35] F. Baccelli, and B. Blaszczyszyn, "Stochastic Geometry and Wireless Networks, Volume I–Theory", *NOW Foundations and Trends in Networking*, vol. 3, no. 3–4, 2009, pp.150.

[36] F. Baccelli, and B. Blaszczyszyn, "Stochastic geometry and wireless networks: Volume II Applications", *NOW Foundations and Trends in Networking*, vol. 4, no. 1–2, Jan. 2010, pp. 1–312.

[37] F. Martin-Vega, F. Lopez-Martinez, G. Gomez, and M. Aguayo-Torres, "Multi-user coverage probability of uplink cellular systems: A stochastic geometry approach", *In IEEE Global Communications Conference*, Austin, Dec. 2014, pp. 3989–3994.

[38] L. Wang, and V. Fodor, "On the gain of primary exclusion region and vertical cooperation in spectrum sharing wireless networks", *IEEE Transactions on Vehicular Technology*, vol. 61, no. 8, pp. 3746–3758, Oct. 2012.

[39] F. Zhou, Y. Wu, Y. C. Liang, Z. Li, Y. Wang, and K. K. Wong, "State of the art, taxonomy, and open issues on cognitive radio networks with NOMA", *IEEE Wireless Communications*, vol. 25, no. 2, pp. 100–108, April 2018.

[40] M. Zeng, G. I. Tsiropoulos, O. A. Dobre, and M. H. Ahmed, "Power allocation for cognitive radio networks employing non-orthogonal multiple access", *in IEEE Global Communications Conference (GLOBECOM)*, Washington, Dec. 2016, pp. 1–5.

[41] A. Papoulis and S. U. Pillai, "Probability, random variables, and stochastic processes", New York, NY, USA: McGraw-Hill, 2002.

S.D. Okegbile received B.Tech (Hons.) degree in Computer Engineering (First class division) from Ladoke Akintola University of Technology, Ogbomoso, Nigeria, in 2011 and M.Sc. degree in Computer Science (Distinction) from Obafemi Awolowo University, Ile-Ife, Nigeria, in 2016. He is currently pursuing the Ph.D. degree in Computer Engineering in the Department of Electrical, Electronic and Computer Engineering, University of Pretoria, South Africa. His research interests are in the area of pervasive and mobile computing which includes various interesting topics on cognitive radio networks, internet of things and wireless sensor networks.

B. T. Maharaj received the Ph.D. degree in wireless communications from the University of Pretoria, South Africa. He is currently a Professor and holds the position of Sentech Chair of Broadband Wireless Multimedia Communications with the Department of Electrical, Electronic, and Computer Engineering, University of Pretoria. His research interests are in MIMO channel modelling, OFDM-MIMO systems, and cognitive radio for rural broadband.

Attahiru S. Alfa is Professor Emeritus at the University of Manitoba, Department of Electrical and Computer Engineering and Extraordinary Professor at the University of Pretoria, Department of Electrical, Electronic and Computer Engineering. Dr. Alfa's most recent research focus covers age of information, wireless sensor networks, cognitive radio networks, network restoration tools for wireless sensor networks, and the role of 5G on IoT, with specific interest in the mathematical modeling of those systems. His general research covers, but not limited to, the following areas: queueing theory and applications, optimization, performance analysis and resource allocation in telecommunication systems, modeling of communication networks, analysis of cognitive radio networks, modeling and analysis of wireless sensor networks, and smart cities. Some of his previous works include developing efficient decoding algorithms for LDPC codes, channel modeling, traffic estimation for the Internet, and cross layer analysis. Dr. Alfa also works in the application of queueing theory to other areas such as transportation systems, manufacturing systems and healthcare systems. He has authored two books, "Queueing Theory for Telecommunications: Discrete Time Modelling of a Single Node System", published by Springer in 2010, and "Applied Discrete-Time Queue" published in 2015, also by Springer, as a second edition of the first book; and also co-authored (with Dr. Ibrahim) a book titled: "Optimization Methods for User Admissions and Radio Resource Allocation for Multicasting over High Altitude Platforms" published by River Publishers in 2019.